Journal of Statistical Physics, Vol. 86, Nos. 5/6, 1997

Different Self-Avoiding Walks on Percolation Clusters: A Small-Cell Real-Space Renormalization-Group Study

J.-P. Hovi[1,2] **and Amnon Aharony**[1,3]

Received April 19, 1996; final August 15, 1996

We calculate the average number of steps N for edge-to-edge, "normal," and indefinitely growing self-avoiding walks (SAWs) on two-dimensional critical percolation clusters, using the real-space renormalization-group approach, with small "H" cells. Our results are of the form $N = AL^{D_{SAW}} + B$, where L is the end-to-end distance. Similarly to several deterministic fractals, the fractal dimensions D_{SAW} for these three different kinds of SAWs are found to be equal, and the differences between them appear in the amplitudes A and in the correction terms B. This behavior is attributed to the hierarchical nature of the critical percolation cluster.

KEY WORDS: Percolation clusters; self-avoiding walks; indefinitely growing self-avoiding walks; real-space renormalization group; fractals; universality; corrections to scaling.

1. INTRODUCTION

The statistics of self-avoiding walks (SAWs) on percolation clusters, simulating, e.g., polymers trapped in porous media,[1] has attracted a great deal of interest,[2-6] not only due to physical applications, but also because it is a simple problem of statistical mechanics with quenched random disorder. The SAW is a random walk which is never allowed to intersect itself. Within this constraint one may define different types of SAWs, each having its own set of rules which define the weight associated with the walk. In this paper, we concentrate on three types of SAWs. The first type contains the

[1] Raymond and Beverly Sackler Faculty of Exact Sciences, School of Physics and Astronomy, Tel Aviv University, Ramat Aviv 69978, Tel Aviv, Israel.
[2] Laboratory of Physics, Helsinki University of Technology, 02150 Espoo, Finland.
[3] Department of Physics, University of Oslo, Blindern, N-0316 Oslo 3, Norway.

0022-4715/97/0300-1163$12.50/0 © 1997 Plenum Publishing Corporation

edge-to-edge SAWs, which are all the walks which connect two given points of the structure. The second type is the *indefinitely growing* SAW (IGSAW), which starts at a given point and the walk is "legitimate" only if it is capable of continuing to grow forever from its present endpoint.[7] The third type is the "normal" SAW, which is included in the ensemble whether it can continue to grow forever or not. Obviously, the ensemble of "normal" N-point SAWs contains also all the N-point IGSAWs and the edge-to-edge SAWs.

Previous studies[7-9] of IGSAWs and "normal" SAWs revealed that on the two-dimensional square lattice the average end-to-end distance $\langle L \rangle$ scales as $\langle L \rangle \propto N^{\nu}$, where N is the number of steps and $\nu = 1/D_{\mathrm{SAW}}$ or $1/D_{\mathrm{IGSAW}}$. Interestingly, these authors found a large difference between the fractal dimensions of the different kinds of walks: $D_{\mathrm{SAW}} = 4/3$ and $D_{\mathrm{IGSAW}} = 1.75$. It has been suggested[7,8] that the critical dimension of the problem is $d_c = 3$, above which the fractal dimensions are equal.

One of the theoretical tools which has allowed great advances in the study of SAWs on both regular lattices[10] and on fractal geometries[2-5] is the real space renormalization-group (RG) approach. In this treatment one calculates the averages in the grand-canonical ensemble by assigning a weight factor x to each step of the walk. Thus the weight of a legitimate N-step walk becomes x^N. This yields a fixed point x^*,[5] at which the average number of the steps in the SAW behaves as a power law, $N \propto L^{D_{\mathrm{SAW}}}$, where L is the end-to-end distance of the walk.

In a recent paper, Shussman and Aharony[11] used this technique to investigate the three types of SAWs on several deterministic fractal structures, such as the Mandelbrot–Given (MG) curve.[12] Like critical percolation clusters, these fractals have a finite order of ramification. They found that the average number of steps behaves asymptotically as $N = AL^{D_{\mathrm{SAW}}} + B$. Remarkably, in contrast to regular lattices, all three kinds of walks were found to have the same fractal dimension on a given deterministic fractal. However, the amplitudes A and the correction terms B differed among the types of SAWs.

In this paper, we extend the analysis to randomly diluted fractals at the percolation threshold. At the threshold, the critical percolation clusters are statistically self-similar.[13] Therefore, they can be described by the renormalization group. Here we use an approximate real-space RG, called the "H-cell" RG, which turned out to be very accurate for bond percolation on the square lattice.[14,15] It has also given excellent results for the permeability of oil reservoirs away from the percolation threshold.[16]

Analyzing the different kinds of SAWs with the "H-cell" RG, we find very similar results to those for the deterministic fractals, especially for the MG curve. Specifically, the final expression for the SAW average length has

the same exponent for all three SAWs, and the differences appear in the amplitudes and correction terms.

The rest of the paper is organized as follows. In the next section we summarize briefly the details of the analytical method, together with some preliminary results. The expressions for the average number of steps for the IGSAWs and normal SAWs are worked out in Section 3. The paper concludes in Section 4.

2. ANALYTICAL METHOD

For simplicity, we discuss two-dimensional (2D) percolation, and consider a 2×2 "H-cell" as shown in Fig. 1a. In the RG transformation, the eight bonds in the cell are replaced by a "renormalized" cell with only two bonds, which represent connectivity in the horizontal and vertical directions. Considering the horizontal spanning, and ignoring the dangling bonds, one realizes that the horizontal connectivity is determined by five bonds. Given that each of these five bonds has a probability p (or $1-p$) to be occupied (or vacant), the resulting configurations are displayed in Fig. 1b together with their probabilities. The sum of these probabilities yields the renormalized probability of the new bond,[14, 13]

$$p' = R(p) = 2p^5 - 5p^4 + 2p^3 + 2p^2 \tag{1}$$

A direct calculation shows that the nontrivial fixed point is $p^* = p_c = 1/2$, as it should be for the bond problem. One of the advantages of the "H-cell" is that this result holds for a general $L \times L$ cell.[15]

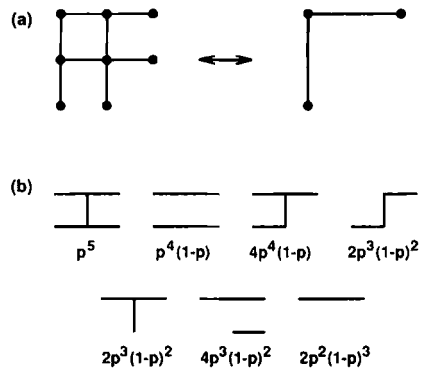

Fig. 1. (a) A 2×2 "H-cell" with eight bonds (left) and a renormalized cell with only two bonds (right); (b) generic parts of the original cell, which contribute to the horizontal spanning.

Following ref. 5, we can then study the SAWs on this structure by assigning an energy ε to each occupied bond which also contains the SAW. The statistical weight associated with each bond in the SAW thus becomes $x = \exp[-(\varepsilon - \mu)/T]$, where T is the temperature and μ is the chemical potential per single occupied bond. In this context x is called the fugacity per bond, generalizing the ordinary definition of the fugacity $[\exp(\mu/T)]$. In the grand-canonical ensemble, the partition function Z is given by summing the statistical weights of all the legitimate SAWs (given the type of SAW of interest) of all the lengths N,

$$Z = \sum_{\text{SAWs}} x^N \tag{2}$$

where Z is the partition function of a specific realization of the quenched random occupation of bonds. For a finitely ramified fractal, Z can be calculated iteratively. In this case, the right-hand side of Eq. (2) can be written as a sum over SAWs which walk over renormalized bonds, and the renormalized fugacity x' for SAWs on each such bond is found by a similar equation, $x' = \sum x^N$, with the sum running over edge-to-edge SAWs inside this bond.[11] This procedure is more complicated in the *random* case, when different bonds may have different fugacities.[17] In that case, each factor x^N is replaced by a product of (potentially) different fugacities, and one should follow the full distribution function of the fugacities. Le Doussal and Machta[5] followed this route numerically, and found a flow toward a "zero-temperature" fixed point of the distribution. However, the numerical values they found for ν were quite close to those found by a simpler approximate approach, which can be carried out analytically. In this approach, used by Meir and Harris,[4] one follows only the iterated values of the *average* occupied bond "free energy" $\langle \log(x) \rangle$. This approximation is in the same spirit as done, e.g., for the conductance of dilute resistor networks,[15, 13] where excellent results were obtained by replacing the distribution function of the bond conductances by two delta functions, at zero (with probability $1-p$) and at the renormalized bond average conductance. In many respects, the distribution function of $\log(x)$ looks like those of other geometrical cluster properties, e.g., the minimal path between pairs of points on the cluster. As we showed elsewhere,[18] the scaling of the average property (or, equivalently, of the location of the peak of the distribution) does follow the same recursion relations found by such an approximation (although the width also increases under iteration). Since our main purpose here is not to obtain exact exponents, but rather to compare several different types of SAWs, we believe that treating all these types within the same

approximate scheme will still give a reliable answer concerning their relative behavior.

All possible edge-to-edge SAWs on the 2×2 "H-cell" are classified in Fig. 2. Summing over the different configurations of the original cell, we find the recursion relation for the average free energy $\log(x)$,[4]

$$\begin{aligned} p' \log(x') &= \sum (\text{probability of configuration}) \times \log(Z) \\ &= \log(x)[6p^5 - 14p^4 + 6p^3 + 4p^2] \\ &\quad + \log(1+x)[-3p^5 + 4p^4] + \log(2)[p^4] \end{aligned} \tag{3}$$

Analyzing this recursion relation at $p' = p = p^* = 1/2$, one finds the fixed point corresponding to the SAWs at the percolation threshold: ($p^* = 1/2$, $x^* \approx 0.787877$).

The average length of the edge-to-edge SAWs is given by taking the derivative of the free energy in the nth generation, $F_n = -T \log(x_n)$, with respect to the chemical potential,

$$\langle N \rangle_n = -\frac{\partial F_n}{\partial \mu} = \frac{\partial \log(x_n)}{\partial \log x}\bigg|_{x = x^*} \tag{4}$$

The fractal dimension associated with the SAWs can then be determined by calculating how the average SAW length increases during each step of the RG transformation. The average number of bonds in the SAW scales asymptotically as $\langle N \rangle \propto L^{D_{\mathrm{SAW}}}$. Since the end-to-end length in the nth

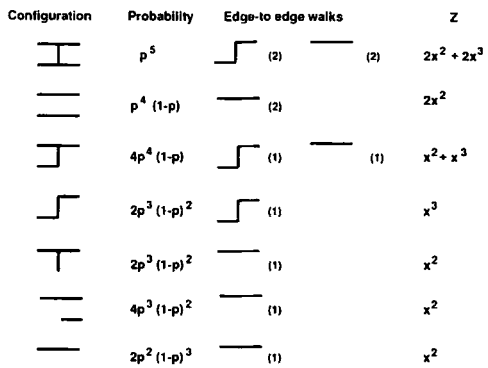

Fig. 2. All the edge-to-edge SAWs on various configurations of the 2×2 "H-cell." The numbers in parantheses indicate how many times such a walk occurs. Each bond of the walk has fugacity x, and $Z = \sum_{\mathrm{SAW}} x^N$.

generation is $L=b^n$, where b is the length rescale factor (here $b=2$), we conclude that

$$D_{\mathrm{SAW}}=\lim_{n\to\infty}\frac{\log(\langle N\rangle_{n+1}/\langle N\rangle_n)}{\log(b)} \tag{5}$$

Using Eq. (4) at the critical point (p^*, x^*), we find that

$$\langle N\rangle_{n+1}/\langle N\rangle_n=\left.\frac{\partial\log(x')}{\partial\log(x)}\right|_{x=x^*}\equiv m \tag{6}$$

Specifically, applying the procedure above to the edge-to-edge SAWs, we find from Eq. (3) that

$$m=\left.\frac{\partial\log(x')}{\partial\log(x)}\right|_{x=x^*}=\frac{34}{16}+\frac{5}{16}\frac{x^*}{1+x^*}\approx 2.2627 \tag{7}$$

yielding $D_{\mathrm{SAW}}\approx 1.178$. Using Eq. (4), we find that the final expression for the average number of steps in the SAW is given by

$$\langle N\rangle_n=x^*\left.\frac{\partial\tilde{F}_n}{\partial x}\right|_{x=x^*}=\left.\frac{\partial\tilde{F}_n}{\partial\tilde{F}_{n-1}}\cdots\frac{\partial\tilde{F}_1}{\partial\log x}\right|_{x=x^*}=m^n=L^{D_{\mathrm{SAW}}} \tag{8}$$

where $\tilde{F}_n\equiv\log(x_n)$. Thus, the amplitude for the edge-to-edge SAWs on the "H-cell" RG is equal to one, and there are no corrections to scaling. A similar situation was encountered previously[11] for the MG curve, with a slightly different fractal dimension for the edge-to-edge SAWs (the MG curve yields $D_{\mathrm{SAW}}\approx 1.206$).

3. DIFFERENT TYPES OF SAWS ON THE "H-CELL" RG

In this section we calculate the expressions for the average number of steps, considering IGSAWs and normal SAWs in the nth generation of the RG transformation. We limit ourselves to the "H-cell" RG, thus counting only those SAWs which enter the RG cell of Fig. 1a through one edge (e.g., the left vertical edge) and either leave the cell through the opposite edge or end inside the bulk of the cell, but excluding those SAWs which touch the lower edge of the cell. This is based on the basic spirit of the "H-cell" RG. This procedure actually maps the original lattice onto a hierarchical structure, whose backbone is built on the basic "Wheatstone bridge": the basic "H" is replaced by a bridge, as in Fig. 3a, and then each bond on the bridge is replaced by a smaller bridge, and so on. The transverse bonds

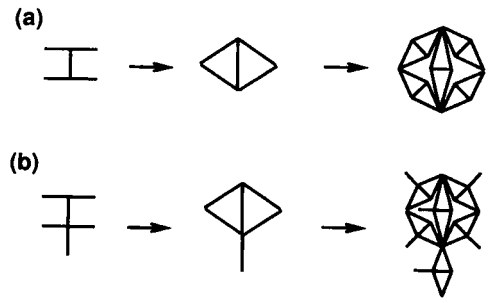

Fig. 3. Hierarchical structure for (a) the backbone, (b) with a dangling bond.

then play the role of dangling bonds, or dead ends (Fig. 3b).[13] Experience shows[13, 18] that this hierarchical structure imitates the physical properties of the original lattice very well.

As far as the IGSAWs are concerned, we can ignore the dangling bonds altogether, since the walks must be able to leave the structure from the right edge. In principle, for the "normal" SAWs, dangling bonds could have some effect, and we discuss them further below.

3.1. IGSAWs on the "H-Cell" RG

The ensemble used above to analyze the edge-to-edge SAWs becomes unsuitable for such self-avoiding walks, which do not have to span between the ends of the basic iteration. We define an ensemble for IGSAWs by generalizing the grand canonical ensemble and taking into account all the walks that start at an edge of a fractal generation and end either inside the bulk or span to the other edge. Since the edge-to-edge distance L is still a characteristic linear size for the SAWs, we continue to use it for our scaling expressions. Thus we find the recursion relation for the free energy of the IGSAWs in the first generation of the RG, $\tilde{I}_1$, by considering all the possible IGSAWs in various configurations of the "H-cell" (see Fig. 4)

$$\begin{aligned} p'\tilde{I}_1 &= \dot{\sum}\,(\text{probability of configuration}) \times \log(Z) \\ &= \log(x)[p'] + \log(1+x)[p' + p^5 - 2p^3(1-p)^2] \\ &\quad + \log(2)[p^4(1-p) + p^5] + \log(2+2x+x^2)[2p^4(1-p)] \\ &\quad + \log(1+x+x^2)[2p^3(1-p)^2] \end{aligned} \tag{9}$$

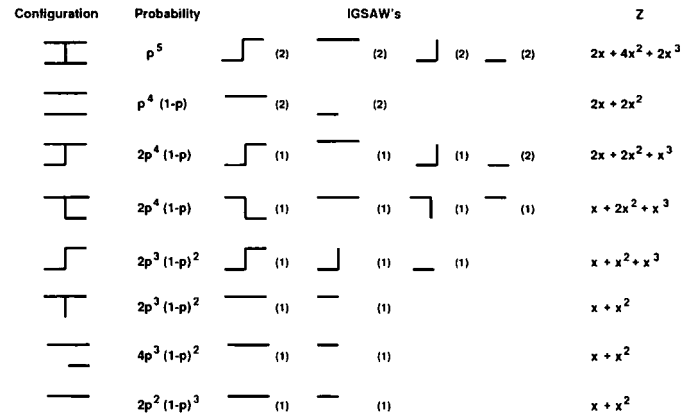

Fig. 4. All the IGSAWs on various configurations of the 2×2 "H-cell." The walks enter the cell from the left.

The recursion relation for the next generations can be written down by observing that legitimate IGSAWs for the $(n+1)$th generation have to span from edge to edge in the nth generation and subsequently be indefinitely growing in the $(n+1)$th generation. Therefore each N-step walk of Fig. 4 carries a statistical weight $x_n^{N-1} i_n$, where $\tilde{F}_n = \log(x_n)$ and $\tilde{I}_n = \log(i_n)$ are the free energies associated with nth-generation edge-to-edge SAWs and IGSAWs, respectively. Inspecting the walks classified in Fig. 4, we find that

$$\tilde{I}_{n+1} = \tilde{I}_n + \tilde{I}_1(\tilde{F}_n) - \tilde{F}_n \tag{10}$$

This expression is again similar to that found for the MG curve in ref. 11.

The next step is to calculate the average length of IGSAWs in the $(n+1)$th generation, which can be calculated from the derivative of the corresponding free energy [see Eq. (4)]. Using Eqs. (10) and (8) and the chain rule, we find that

$$\langle N_I \rangle_{n+1} \equiv x \frac{\partial \tilde{I}_{n+1}}{\partial x} = \langle N_I \rangle_n + [\langle N_I \rangle_1 - 1] m^n$$

$$= \frac{\langle N_I \rangle_1 - 1}{m-1} m^{n+1} + \frac{m - \langle N_I \rangle_1}{m-1} \tag{11}$$

where $m \approx 2.2627$, defined in Eq. (6), has the same value as before. At the critical point one finds from Eq. (9) that

$$\begin{aligned}\langle N_I \rangle_1 &\equiv \left.\frac{\partial \tilde{I}_1}{\partial \log(x)}\right|_{x=x^*} \\ &= \left[1 + \frac{15}{16}\frac{x}{1+x} + \frac{1}{8}\frac{2x(1+x)}{2+2x+x^2} + \frac{1}{8}\frac{x(1+2x)}{1+x+x^2}\right]\Bigg|_{x=x^*} \\ &\approx 1.6024 \end{aligned} \tag{12}$$

Combining Eqs. (9) and (11), we get our final expression for the average length of legitimate IGSAWs,

$$\langle N_I \rangle_{n+1} = 0.4770 L^{D_{\mathrm{IGSAW}}} + 0.5230 \tag{13}$$

where $D_{\mathrm{IGSAW}} = D_{\mathrm{SAW}} = \log(m)/\log(2) \approx 1.178$.

In conclusion, we find that the fractal dimension for the IGSAWs is equal to that of the edge-to-edge SAWs, but the amplitudes differ and the IGSAWs have a constant correction term. We should note again that similar results were found for the Mandelbrot–Given curve[11] with only minor differences in the numerical factors.

3.2. Normal SAWs on the "H-Cell" RG

In this subsection we use a similar method to analyze the normal SAWs, which are included in the ensemble whether they can grow indefinitely or not. In addition to the edge-to-edge walks (see Fig. 2), the normal SAWs also include those ending inside the bulk. At first we count only those SAWs which do not enter the dangling ends, as listed in Fig. 5. Considering the first generation of the RG transformation, we find that the free energy $\tilde{S}_1$ is given by

$$\begin{aligned} p'\tilde{S}_1 = {} & \log(x)[p'] + \log(1+x)[2p^2(1-p)^3 + 2p^3(1-p)^2 + 5p^4(1-p)] \\ & + \log(2+x)[2p^3(1-p)^2] + \log(1+2x)[2p^3(1-p)^2] \\ & + \log(2)[p^4(1-p)] + \log(1+x+x^2)[2p^3(1-p)^2] \\ & + \log(2+3x+2x^2)[2p^4(1-p)] \\ & + \log(2+4x+3x^2)[p^5] \end{aligned} \tag{14}$$

The recursion relation of the free energy in the following generations can be written down in terms of the free energies of all the normal walks

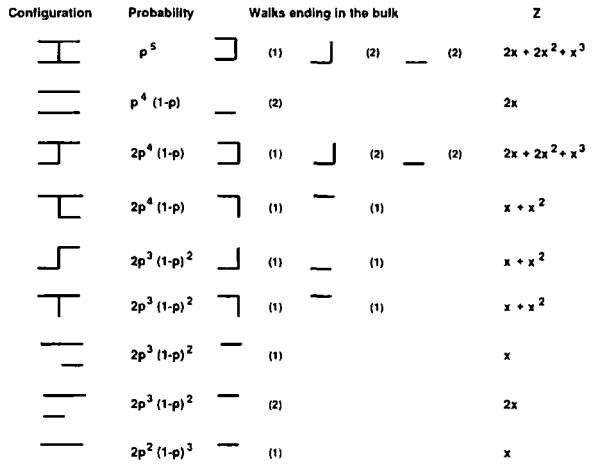

Fig. 5. All the SAWs ending inside the bulk on various configurations of the 2×2 "H-cell." The walks enter the cell from the left. The normal SAWs also contain the edge-to-edge ones, shown in Fig. 2.

$[\tilde{S}_n = \log(s_n)]$, edge-to-edge walks $[\tilde{F}_n = \log(x_n)]$, and walks ending in the bulk $[\tilde{C}_n = \log(c_n)]$. Similarly to the previous section, all the N-step walks in Figs. 2 and 5 carry statistical weights $x_n^{N-1} s_n$, except for the two $\sqsupset$-shaped walks in Fig. 5, which contribute $x_n^3 + 2x_n^2 c_n$. Thus we find

$$\begin{aligned} p'\tilde{S}_{n+1} = {} & p'\tilde{S} + p'\tilde{S}_1(\tilde{F}) - p'\tilde{F} \\ & + [2p^4(1-p)] \log(2s + 3sx + sx^2 + x^3 + 2x^2 c) \\ & - [2p^4(1-p)] \log(2s + 3sx + 2sx^2) \\ & + [p^5] \log(2s + 4sx + 2sx^2 + x^3 + 2x^2 c) \\ & - [p^5] \log(2s + 4sx + 3sx^2) \end{aligned} \tag{15}$$

where we have adopted a short-hand notation by dropping the subscripts n on the right-hand side of the equation. Obviously, as the normal SAWs consist of the edge-to-edge walks and those ending inside the bulk, the partition functions for each generation obey the sum rule $s = x + c$.

As previously, we next calculate the average number of steps of all the normal SAWs. Using Eqs. (14) and (15), we find after a straightforward calculation (see Appendix) that in the leading order the average length of all the normal SAWs behaves as

$$\langle N_S \rangle_{n+1} \sim 0.5177 L^{D_{\mathrm{SAW}}} + 0.4000 + 0.1531 L^{-y_1} + 0.0027 L^{-y_2} \tag{16}$$

where $D_{SAW} \approx 1.178$ has the same value as above, while $\vartheta_1 \approx 0.383$ and $\vartheta_2 \approx 1.561$. Thus we find that the normal SAWs also scale with the same fractal dimension as the IGSAWs and the edge-to-edge SAWs, but with different correction-to-scaling terms and with different amplitudes. Again, the results for the MG curve are very similar.[11]

Finally, we need to consider the "normal" SAWs which may end inside the dangling ends (still with the restriction that they do not exit through the lower edge of the cell). The calculation, which involves many more possible paths, is similar to that given in the Appendix. It is easy to see that because every new N-point walk generated by dangling ends carries weight $x_n^{N-1} s_n$, the dangling ends do not yield new kinds of terms for the recursion relation (A1). In particular, we can follow the steps of the Appendix and rederive Eq. (A13), with slightly modified $\langle N_S \rangle_1$, s_1, $g_k (k = 0, 1, 2)$, and q. Such changes affect only amplitudes and the correction-to-scaling terms, but the leading scaling power remains unchanged. For example, using the structure depicted in Fig. 3b, we find

$$\langle N_S \rangle_{n+1} \sim 0.5630 L^{D_{SAW}} + 0.3976 + 0.1028 L^{-0.536} + 0.0023 L^{-1.714} \tag{17}$$

This result is again similar to that of ref. 11, which found that the dangling ends do not change the leading scaling behavior for the MG curve either.

3.3. SAWs on Undiluted "H-Cell"

In order to study the possible reasons for the equal dimensionalities for the different kinds of SAWs, we carried out similar calculations for the undiluted "H-cell," i.e., for the leftmost configuration in the upper row of Fig. 1. The results are thus obtined by simply setting $p' = p = 1$ in all the above recursion relations.

Classifying all the possible edge-to-edge SAWs on that configuration, we find the recursion relation for the average free energy

$$\log(x') = \log(2x^2 + 2x^3) \tag{18}$$

which has the fixed point $x^* = \frac{1}{2}(-1 + \sqrt{3}) \approx 0.36603$. Proceeding similarly to Section 2, we find that

$$m = \frac{\partial \log(x')}{\partial \log(x)}\bigg|_{x = x^*} = \frac{2 + 3x^*}{1 + x^*} \approx 2.2680 \tag{19}$$

which gives $D_{SAW} = \log(m)/\log(2) \approx 1.1814$. Thus we find that within this approximation, the fractal dimension of SAWs on the diluted and undiluted "H-cell" are not very different: 1.178 and 1.181, respectively.

The analysis of IGSAWs and "normal" SAWs is very similar to what we used in the dilute case. Considering all the possible IGSAWs we find (the notation is the same as in Section 3.1)

$$\tilde{I}_1 = \log(2x + 4x^2 + 2x^3) \tag{20}$$

$$\tilde{I}_{n+1} = \tilde{I}_n + \tilde{I}_1(\tilde{F}_n) - \tilde{F}_n \tag{21}$$

This gives

$$\langle N_I \rangle_1 = \left. \frac{1+3x}{1+x} \right|_{x=x^*} \approx 1.5359 \tag{22}$$

$$\langle N_I \rangle_{n+1} = \frac{\langle N_I \rangle_1 - 1}{m-1} m^{n+1} + \frac{m - \langle N_I \rangle_1}{m-1} \tag{23}$$

The latter equation is the same as Eq. (11), and we find

$$\langle N_I \rangle_{n+1} = 0.4226 L^{D_{\mathrm{IGSAW}}} + 0.5774 \tag{24}$$

where $D_{\mathrm{IGSAW}} = D_{\mathrm{SAW}} = 1.181$. The analysis of the normal SAWs is more tedious, but still straightforward, giving the final result

$$\langle N_S \rangle_{n+1} \sim 0.5000 L^{D_{\mathrm{SAW}}} + 0.3349 + 0.2401 L^{-\vartheta_1} - 0.0462 L^{-\vartheta_2} \tag{25}$$

where $D_{\mathrm{SAW}} \approx 1.181$ has the same value as above, while $\vartheta_1 = 2 - D_{\mathrm{SAW}} \approx 0.819$ and $\vartheta_2 = 2$.

From this analysis it is obvious that the structure of the problem on the undiluted "H-cell" is the same as that on the diluted cell. In particular, we find that the different SAWs on an "H-cell," diluted or not, possess the same fractal dimensions. In fact, this result could have been anticipated because the hierarchical structures of Fig. 3 can be well considered as special cases of finitely ramified fractals, for which this kind of the behavior appears to be generic.[11] Thus, although the hierarchical structure fails in producing the behavior observed on the square lattice,[7,9] there is room to expect that our results for the different types of SAWs do hold on critical percolation clusters, due to the hierachical nature of these clusters.

4. CONCLUDING REMARKS

Our renormalization group calculation reveals that on the critical percolation clusters the fractal dimensions for the edge-to-edge SAWs, IGSAWs, and "normal" SAWs are equal, and the differences appeal in the amplitudes and in the correction terms.

Our specific calculation for 2D percolation with the 2×2 "H-cell" yielded $D_{SAW} = 1.178$. This estimate from the small cell RG is about 10% lower than recent Monte Carlo estimates, which give $D_{SAW} = 1.29 \pm 0.025$,[6] but the agreement could be improved by increasing the size of the "H-cell," as experience shows in other cases.[18] The main point of our RG calculation is that the mathematical structure of the problem strongly suggests that the equality of dimensions for the different kinds of SAWs may also hold for a general $L \times L$ cell, thus remaining valid in the limit $L \to \infty$, which corresponds to the real percolation clusters, and also in general dimension d. Our brief analysis of the undiluted "H-cell" allows us to identify the origin of this behavior as the hierarchical nature of the critical percolation clusters.

Finally, if is interesting to note the closeness of all our results to those found for the MG curve. That curve seems to capture all the physical properties of 2D critical percolation clusters.

APPENDIX

In this Appendix we go through the steps leading to Eq. (16).

Substituting Eq. (15) in the definition of the average length, we find that ($p' = p = 1/2$)

$$\begin{aligned} \langle N_S \rangle_{n+1} \equiv x \frac{\partial \tilde{S}_{n+1}}{\partial x} &= x \frac{\partial \tilde{S}_n}{\partial x} + x \frac{\partial \tilde{S}_1(\tilde{F}_n)}{\partial x} - x \frac{\partial \tilde{F}_n}{\partial x} \\ &+ \frac{2}{16} x \frac{\partial}{\partial x} \log \left[1 + \frac{x_n^2 (s_n - x_n)}{s_n \alpha_1(x_n)} \right] \\ &+ \frac{1}{16} x \frac{\partial}{\partial x} \log \left[1 + \frac{x_n^2 (s_n - x_n)}{s_n \alpha_2(x_n)} \right] \end{aligned} \tag{A1}$$

where

$$\alpha_1(x_n) = 2 + 3x_n + 2x_n^2 \tag{A2}$$

$$\alpha_2(x_n) = 2 + 4x_n + 3x_n^2 \tag{A3}$$

Observing that

$$m'' = x \frac{\partial \tilde{F}_n}{\partial x} = \frac{\partial \log(x_n)}{\partial \log(x)} \tag{A4}$$

$$\langle N_S \rangle_n = x \frac{\partial \tilde{S}_n}{\partial x} = \frac{\partial \log(s_n)}{\partial \log(x)} \tag{A5}$$

we can evaluate the derivatives in Eq. (A1), e.g.,

$$x\frac{\partial \tilde{S}_1(\tilde{F}_n)}{\partial x}=\frac{\partial \log s_1(x_n)}{\partial \log x_n}\frac{\partial \log x_n}{\partial \log x}=\langle N_S\rangle_1 m''$$

and find that

$$\begin{aligned}\langle N_S\rangle_{n+1}=\langle N_S\rangle_n&\left[1+\frac{1}{16}\frac{2x^3}{\alpha_1 s+x^2(s-x)}+\frac{1}{16}\frac{x^3}{\alpha_2 s+x^2(s-x)}\right]\\&+[\langle N_S\rangle_1-1]\,m''+\frac{1}{16}m''\\&\times\left[\frac{-2\alpha_1 x^3+4\alpha_1(s-x)\,x^2-2(s-x)\,x^2(3x+4x^2)}{\alpha_1[\alpha_1 s+x^2(s-x)]}\right.\\&\left.+\frac{-\alpha_2 x^3+2\alpha_2(s-x)\,x^2-(s-x)\,x^2(4x+6x^2)}{\alpha_2[\alpha_2 s+x^2(s-x)]}\right]\end{aligned}\tag{A6}$$

where we have dropped the subscripts n on the right-hand side of the equation.

In order to evaluate Eq. (A6) at the fixed point where $x_n=x^*$ for all n, we study first how s_n behaves as a function of n. From Eq. (15) we find that at the fixed point ($p^*=1/2$, $x^*=0.787877$)

$$\begin{aligned}s_n=s_{n-1}&[(2+3x+3x^2-x^3/s_{n-1})^2\,(1+x)^8\,(2+x)^2\,(2+2x)\\&\times(1+2x)^2\,(2+4x+4x^2-x^3/s_{n-1})(1+x+x^2)^2]^{1/16}|_{x=x^*}\end{aligned}\tag{A7}$$

Ignoring the terms $x^3/s_{n-1}\approx 0$, one finds

$$s_n\approx s_{n-1}q\approx s_1 q^{n-1}\tag{A8}$$

where $q\approx 2.950847$. From Eq. (14) one gets that at x^*, $s_1\equiv\exp(\tilde{S}_1)\approx 2.282450$, and $\langle N_S\rangle_1\equiv x\,\partial\tilde{S}_1/\partial x\approx 1.634353$.

Having found that at the fixed point s_n diverges geometrically as a function of n, we turn back to Eq. (A6) and expand the right-hand side in powers of $1/s_n$. We find that

$$\langle N_S\rangle_{n+1}=\langle N_S\rangle_n\left(1+g_1\frac{1}{s_n}\right)+m''\left(\langle N_S\rangle_1-1+g_0+g_2\frac{1}{s_n}\right)+\mathcal{O}\left(\frac{1}{s_n^2}\right)\tag{A9}$$

where all the functions g depend only on x_n and are numbers at $x_n = x^*$:

$$g_0 = \frac{1}{16}\left[\frac{2x^2(2\alpha_1 - 3x - 4x^2)}{\alpha_1(\alpha_1 + x^2)} + \frac{2x^2(\alpha_2 - 2x - 3x^2)}{\alpha_2(\alpha_2 + x^2)}\right]$$

$$\approx 0.019331 \tag{A10}$$

$$g_1 = \frac{1}{16}\left(\frac{2x^3}{\alpha_1 + x^2} + \frac{x^3}{\alpha_2 + x^2}\right)$$

$$\approx 0.013823 \tag{A11}$$

$$g_2 = \frac{1}{16}\left[\frac{6x^3(-\alpha_1 + x + x^2)}{(\alpha_1 + x^2)^2} + \frac{x^3(-3\alpha_2 + 4x + 5x^2)}{(\alpha_2 + x^2)^2}\right]$$

$$\approx -0.027610 \tag{A12}$$

Substituting Eq. (A9) iteratively into itself and using Eq. (A8), we find that

$$\begin{aligned}\langle N_S\rangle_{n+1} &= \langle N_S\rangle_1\left(1 + \frac{g_1}{s_1}\sum_{j=0}^{n-1}\frac{1}{q^j}\right) \\ &\quad + [\langle N_S\rangle_1 - 1 + g_0]\sum_{j=1}^{n} m^j + g_2\frac{q}{s_1}\sum_{j=1}^{n}\left(\frac{m}{q}\right)^j + \mathcal{O}\left(\frac{1}{q^{n+1}}\right) \\ &= \frac{\langle N_S\rangle_1 - 1 + g_0}{m-1}m^{n+1} \\ &\quad \times\left[\left(1 + \frac{g_1}{s_1}\frac{q}{q-1}\right)\langle N_S\rangle_1 - [\langle N_S\rangle_1 - 1 + g_0]\frac{m}{m-1}\right. \\ &\quad \left. + g_2\frac{m}{s_1}\frac{1}{1-(m/q)}\right] \\ &\quad - g_2\frac{q}{s_1}\frac{1}{1-(m/q)}\left(\frac{m}{q}\right)^{n+1} + g_1\frac{q^2}{s_1(1-q)}\left(\frac{1}{q}\right)^{n+1}\end{aligned} \tag{A13}$$

Substituting the numerical values, we get the final expression, i.e. Eq. (16), for the average length of all the SAWs, with $D_{\mathrm{SAW}} = \log(m)/\log(2) \approx 1.178$, $\vartheta_1 = \log(m/q)/\log(2) \approx -0.383$, and $\vartheta_2 = \log(1/q)/\log(2) \approx -1.561$.

ACKNOWLEDGMENTS

J.-P.H. gratefully acknowledges financial support from the Neste Foundation, Emil Aaltonen Foundation, and Finnish Cultural Foundation. This project was also supported by grants from the U.S.–Israel Binational Science Foundation (BSF) and the German–Israeli Foundation (GIF).

REFERENCES

1. H. Nakanishi, In *Annual Reviews of Computational Physics*, Vol. 1 (World Scientific, Singapore, 1994), p. 219.
2. D. Dhar, *J. Math. Phys.* **19**:5 (1978).
3. R. Rammal, G. Toulouse, and J. Vannimenus, *J. Phys.* (Paris) **45**:389 (1984).
4. Y. Meir and A. B. Harris, *Phys. Rev. Lett.* **63**:2819 (1989).
5. P. Le Doussal and J. Machta, *J. Stat. Phys.* **64**:541 (1991).
6. K. Y. Woo and S. B. Lee, *Phys. Rev. A* **44**:999 (1991); P. Grassberger, *J. Phys. A* **26**:1023 (1993); M. D. Rintoul, J. Moon, and H. Nakanishi, *Phys. Rev. E* **49**:2790 (1994).
7. K. Kremer and J. W. Lyklema, *Phys. Rev. Lett.* **54**:267 (1985).
8. K. Kremer and J. W. Lyklema, *J. Phys. A* **18**:1515 (1985).
9. A. Weinrib and S. A. Trugman, *Phys. Rev. B* **31**:2993 (1985).
10. B. Shapiro, *J. Phys. C* **11**:2829 (1978).
11. Y. Shussman and A. Aharony, *J. Stat. Phys.* **77**:545 (1994).
12. B. B. Mandelbrot and J. A. Given, *Phys. Rev. Lett.* **52**:1853 (1984).
13. D. Stauffer and A. Aharony, *Introduction to Percolation Theory*, rev. 2nd ed. (Taylor and Francis, London, 1994).
14. P. J. Reynolds, H. E. Stanley, and W. Klein, *J. Phys. C* **10**:L167 (1977).
15. J. Bernasconi, *Phys. Rev. B* **18**:2185 (1978).
16. A. Aharony, E. I. Hinrichsen, A. Hansen, J. Feder, T. Jøssang, and H. H. Hardy, *Physica A* **177**:260 (1991).
17. Y. Shussman and A. Aharony, *J. Stat. Phys.* **80**:147 (1995).
18. J.-P. Hovi and A. Aharony, *Fractals* **3**:453 (1995); *Phys. Rev. E*, submitted.